

Thouless and Relaxation Time Scales in Many-Body Quantum Systems

Mauro Schiulaz,¹ E. Jonathan Torres-Herrera,² and Lea F. Santos¹

¹*Department of Physics, Yeshiva University, New York City, NY, 10016, USA*

²*Instituto de Física, Benemérita Universidad Autónoma de Puebla, Apt. Postal J-48, Puebla, 72570, Mexico*

(Dated: December 6, 2019)

Studies of the dynamics of isolated interacting many-body quantum systems are at the forefront of experimental and theoretical physics. A major open question is the identification of the time scales involved in the relaxation process of these systems. Using experimental observables and a realistic interacting many-body quantum system, we unveil three different time scales: a very short time that characterizes the early decay of the initial state and two much longer time scales that increase exponentially with system size. These two are the Thouless time, t_{Th} , and the relaxation time, t_{R} . The Thouless time refers to the point beyond which the dynamics acquires universal features and relaxation happens when the evolution reaches a stationary state. We show that in chaotic systems, $t_{\text{Th}} \ll t_{\text{R}}$, while for systems approaching a many-body localized phase, $t_{\text{Th}} \rightarrow t_{\text{R}}$. Our results are compared with those for random matrices, which corroborates their generality.

There is currently great interest in the dynamics of isolated quantum systems with many interacting particles. This is in part due to the advances of experiments with cold atoms, ion traps, and nuclear magnetic resonance platforms, which allow for the simulation of unitary dynamics of highly tunable Hamiltonians for long times [1–9]. Great efforts have been devoted to conciliate reversible microscopic dynamics and irreversible thermodynamics [10–13]. Increasing attention has also focused on the analysis of the metal-insulator transition [14–16] and the quantum-classical correspondence, specially in the context of many-body quantum chaos and the scrambling of quantum information [17–23]. A missing piece in these studies is a complete framework of all time scales involved in the relaxation to equilibrium.

Several works have discussed what equilibration in closed finite quantum systems actually means [24–29], a subject on which we find consensus. Equilibration refers to the proximity of an observable to its asymptotic value for most times, despite the presence of temporal fluctuations caused by the spectrum discreteness. Much more problematic is the identification of the time scales involved in the relaxation process, for which there are several interesting, but contradictory, results. Some suggest that equilibration happens at very short times, while others indicate just the opposite, that extremely long times are required [10, 30–36].

To properly determine the relaxation time of many-body quantum systems, one needs to have a complete picture of the different behaviors that emerge at different time scales. Without that, one risks reaching misleading conclusions. With the support from random matrices, we have been able to unveil these different time behaviors in realistic many-body quantum systems. This allows us to provide analytical predictions for the time scales of the relaxation process, which are shown to agree extremely well with our exact numerical results.

We consider a one-dimensional local spin-1/2 model with onsite disorder that is taken far from equilibrium. This system can be mapped into models of hardcore bosons and spinless fermions and has been studied ex-

perimentally in the context of many-body localization [7]. Two observables are investigated, the survival probability, which is the squared overlap between the initial state and its time evolved counterpart, and the spin autocorrelation function, which is equivalent to the density imbalance measured in experiments with cold atoms [7]. For small disorder strength, the eigenvalues of the spin model are strongly correlated and comparable to what one finds for full random matrices from a Gaussian orthogonal ensemble (GOE) [37]. This justifies comparing its dynamics with that for GOE matrices.

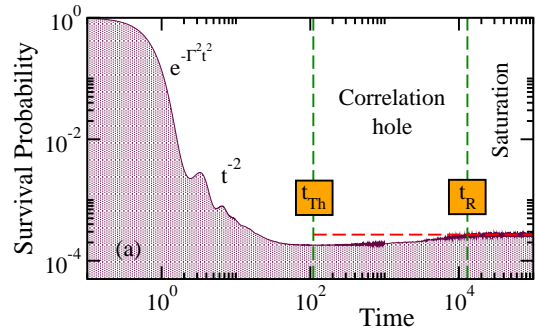


FIG. 1. Different stages of the evolution of the survival probability for the disordered spin-1/2 model in the chaotic regime.

Figure 1 illustrates the entire evolution of the survival probability for the chaotic spin model, from the time it is taking far from equilibrium to the moment it equilibrates. Before the point indicated as t_{Th} , the dynamics depends on the shape and borders of the initial state energy distribution. Initially, the decay is very fast, Gaussian, as in Fig. 1, or exponential, depending on how far out of equilibrium the system is taken [38–40]. The decay rate is given by the width Γ of the energy distribution. Subsequently, a power-law behavior emerges with exponent determined by the bounds of the spectrum [41, 42].

Beyond t_{Th} , the dynamics becomes universal and analogous to what one has for random matrices. This is equivalent to what happens in noninteracting disordered

quantum systems, where t_{Th} is called Thouless time, so the same designation is used here. In the evolution of chaotic systems with discrete spectra, correlations between the eigenvalues are resolved at t_{Th} and they lead to a dip below the saturation point, known as correlation hole [43–47]. This dip has been recently studied in local many-body Hamiltonians [42, 48, 49] and in the Sachdev-Ye-Kitaev model [19–21]. It is not exclusive to the survival probability, but develops also in experimental observables, such as the spin autocorrelation function [42, 49].

The dynamics finally saturates at the point indicated as t_{R} in Fig. 1, referred to as the relaxation time. After t_{R} , the observable just fluctuates around its infinite-time average (horizontal dashed line).

As evident in Fig. 1, the characteristic time $1/\Gamma$ is much smaller than t_{Th} and t_{R} . We find that for realistic chaotic models, $t_{\text{Th}} \propto D^{2/3}/\Gamma$, where D is the dimension of the Hilbert space, while $t_{\text{R}} \propto D/\Gamma$. This implies that $t_{\text{Th}} \ll t_{\text{R}}$ and the gap between the two increases with system size. Our results for the survival probability and for the spin autocorrelation function are similar.

As the disorder strength increases, the spin model leaves the chaotic domain and approaches a many-body localized phase, where the eigenvalues are no longer correlated. This affects the dynamics before [50] and after [48] the Thouless time. We show that t_{Th} grows exponentially with the disorder strength, gradually shrinking the correlation hole until its complete disappearance, when $t_{\text{Th}} \sim t_{\text{R}}$.

Models and Observables.— The systems studied here are described by a Hamiltonian $H = H_0 + JV$, where $\hbar = 1$, H_0 is the noninteracting part, V represents the couplings, and J is the coupling strength chosen equal to 1. The eigenvalues and eigenstates of H are E_α and $|\psi_\alpha\rangle$.

For the GOE model, H_0 is the diagonal part of a real and symmetric random matrix H , and V contains the off-diagonal elements. The elements are random numbers from a Gaussian distribution with variance 2 for H_0 and 1 for V . The model is unrealistic, due to the simultaneous interaction of all particles, but its advantage is being analytically tractable.

For the disordered spin-1/2 Hamiltonian, we have

$$H_0 = \sum_{k=1}^L h_k S_k^z \quad \text{and} \quad V = \sum_{k=1}^L \vec{S}_k \cdot \vec{S}_{k+1}, \quad (1)$$

where $S_k^{x,y,z}$ are the spin operators on site k and L is the size of the chain. The amplitudes h_k are uniform random numbers in $[-h, h]$. The model conserves the total magnetization $\mathcal{S}^z = \sum_k S_k^z$. We work with the largest subspace $\mathcal{S}^z = 0$, where strong chaos can be reached [51] and where the dimension of the Hilbert space is $D = L!/(L/2)!^2$. For $h = 0$, the model is integrable [52]. At a critical value h_c , it transitions to a many-body localized phase, where the eigenvalues are uncorrelated. We consider disorder strengths $0.5 \leq h < h_c$, where the energy level have some degree of correlation.

Strong chaos happens at $h \sim 0.5$.

The system is prepared in an eigenstate $|\Psi(0)\rangle$ of H_0 with energy $E_{\text{ini}} = \langle \Psi(0) | H | \Psi(0) \rangle$ away from the edges of the spectrum. The initial state spreads in the many-body basis defined by H_0 due to the strong perturbation V that takes it far from equilibrium.

The two observables studied are the survival probability and the spin autocorrelation function,

$$P_S(t) = |\langle \Psi(0) | e^{-iHt} | \Psi(0) \rangle|^2 = \left| \int \rho_{\text{ini}}(E) e^{-iEt} dE \right|^2, \quad (2)$$

$$I(t) = \frac{4}{L} \sum_{k=1}^L \langle \Psi(0) | S_k^z e^{iHt} S_k^z e^{-iHt} | \Psi(0) \rangle, \quad (3)$$

respectively. The first gives the probability to find the system still in the initial state at time t . It is the square of the Fourier transform of the energy distribution $\rho_{\text{ini}}(E) = \sum_\alpha |\langle \psi_\alpha | \Psi(0) \rangle|^2 \delta(E - E_\alpha)$ of width Γ [40]. It is related to the spectral form factor. The second quantifies how close the spin configuration at time t is to the initial one.

Analytical Results for the GOE Model— For large D , the analytical expression for the entire evolution of the survival probability under GOE matrices is given by [49]

$$P_S(t) = \frac{1 - \overline{P_S}}{D - 1} \left[D \frac{\mathcal{J}_1^2(2\Gamma t)}{(\Gamma t)^2} - b_2 \left(\frac{\Gamma t}{2D} \right) \right] + \overline{P_S}, \quad (4)$$

where $\overline{P_S} \simeq 3/D$ is the asymptotic value, $\mathcal{J}_1(t)$ is the Bessel function of the first kind, $\Gamma = \sqrt{D}$, the two-level form factor is $b_2(t) = [1 - 2t + t \ln(1 + 2t)]\Theta(1 - t) + \{t \ln[(2t + 1)/(2t - 1)] - 1\}\Theta(t - 1)$, and Θ the Heaviside step function. The $b_2(t)$ function describes the correlation hole, the above mentioned dip below $\overline{P_S}$.

Illustrations for $P_S(t)$ for the GOE model are provided in the Appendix (see also [49]). The evolution is initially controlled by $\mathcal{J}_1^2(2\Gamma t)/(\Gamma t)^2$, which at very short times is $\propto 1 - \Gamma^2 t^2$ and later leads to oscillations that decay as t^{-3} . $P_S(t)$ decays up to the minimum of the correlation hole at $t_{\text{Th}}^{\text{GOE}}$ [53]. Beyond the power-law decay, $P_S(t)$ is dominated by $b_2(t)$ and increases toward saturation. The initial growth is linear, $b_2(t) \sim 1 - 2t + \mathcal{O}(t^2)$.

Combining the behaviors immediately before and after $t_{\text{Th}}^{\text{GOE}}$, one can estimate this time scale by imposing $\frac{dP_S(t)}{dt} \Big|_{t=t_{\text{Th}}^{\text{GOE}}} = 0$. In the fully connected GOE model, all factors that depend on D cancel out, resulting in (see Appendix)

$$t_{\text{Th}}^{\text{GOE}} = \left(\frac{3}{\pi} \right)^{1/4} \frac{\sqrt{D}}{\Gamma} = \left(\frac{3}{\pi} \right)^{1/4}. \quad (5)$$

While the initial decay determined by Γ gets faster with D , the subsequent power-law decay lasts for longer, which leads to the constant value of $t_{\text{Th}}^{\text{GOE}}$. At $t = t_{\text{Th}}^{\text{GOE}}$, the survival probability reaches the minimum value $2/D$.

To estimate the relaxation time, we use the asymptotic expansion of the two-level form factor, $b_2(t) \sim t^{-2}$, and

compute the time t_R at which the relative difference between $P_S(t)$ and \overline{P}_S is smaller than a small value δ (see Appendix). This gives

$$t_R \propto \frac{D}{\Gamma\sqrt{\delta}}. \quad (6)$$

The relaxation time is therefore inversely proportional to the mean level spacing Γ/D . This is the definition of the Heisenberg time. Unlike $t_{\text{Th}}^{\text{GOE}}$, the time to reach actual saturation diverges with D .

Time Scales for the Spin Model.— The survival probability for the chaotic spin model is very well described by the following expression [49],

$$P_S(t) = \frac{1 - \overline{P}_S}{D - 1} \left[D \frac{e^{-\Gamma^2 t^2}}{(\Gamma t)^2} g(t) - b_2 \left(\frac{\Gamma t}{2D} \right) \right] + \overline{P}_S, \quad (7)$$

where $g(t) = [(\Gamma t)^2 + A(e^{\Gamma^2 t^2} - 1)]/(1 + A)$ and A is a fitting constant. This expression captures all different behaviors shown in Fig. 1 and can be used to estimate t_{Th} and t_R . Contrary to full random matrices, the interactions in physical systems are often two-body and local, resulting in very sparse Hamiltonian matrices and $\Gamma \propto \sqrt{L}$ [39]. However, the correlation hole is described by the same b_2 function used in the GOE model. Up to the minimum of the hole at t_{Th} , the evolution depends on the model and observable, but beyond that, the dynamics are universal.

Analogously to the derivation of $t_{\text{Th}}^{\text{GOE}}$, we combine the two behaviors at the vicinity of the minimum of $P_S(t)$, namely the power-law decay $\propto t^{-2}$ and the subsequent linear increase of $b_2(t)$, and find that

$$t_{\text{Th}} \propto \frac{D^{2/3}}{\Gamma} \sim \frac{e^{2L \ln(2)/3}}{\sqrt{L}}. \quad (8)$$

The Thouless time for realistic chaotic many-body quantum systems increases exponentially with system size. This happens because here $\Gamma \propto \sqrt{L}$, instead of $\propto \sqrt{D}$, but the power-law behavior still extends with D .

Figure 2 (a) shows $P_S(t)$ for different system sizes, making evident the growth of t_{Th} with L . The explicit dependence is studied in Fig. 2 (b), where the prediction from Eq. (8) is confirmed (see circles and solid line). While the characteristic time $1/\Gamma$ for the initial decay of $|\Psi(0)\rangle$ decreases with system size, the time for detecting the eigenvalues correlations increases exponentially with L . If the analysis of the dynamics focuses only on the initial fast decay, one might incorrectly conclude that larger systems equilibrate faster.

At t_{Th} , the spread of the initial state in the many-body space defined by the H_0 -basis is complete and the remaining dynamics is due only to the dephasing of the level spacings, being therefore fully quantum in nature. The procedure to obtain the relaxation time is equivalent to what was done for the GOE model and Eq. (6) is recovered. This is validated with the numerical results

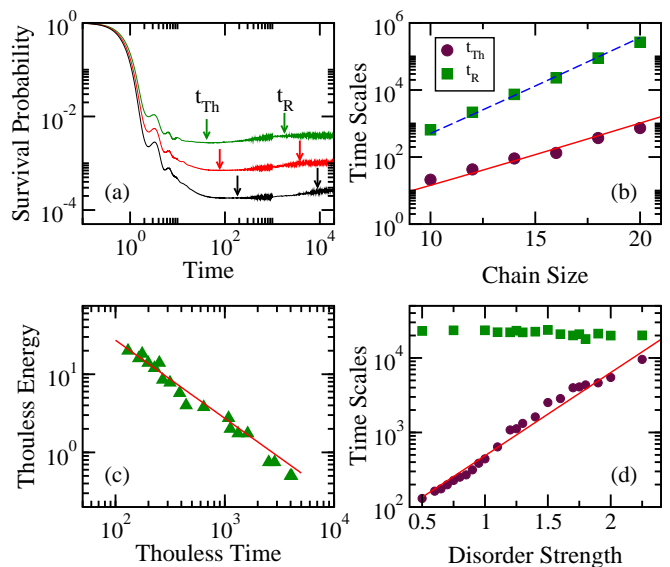


FIG. 2. Survival probability vs time (a); Thouless time and relaxation time as a function of system size (b) and disorder strength (d); escape point from the logarithmic level number variance vs t_{Th} (c). Circles are for t_{Th} and squares for t_R . In (b): solid line is for Eq. (8) and dashed line for Eq. (6). In (c) and (d): solid line is for the fit $E_{\text{Th}} = 2724/t_{\text{Th}}$ and $t_{\text{Th}} \sim 37e^{2.6h}$, respectively. In (a): $L = 12, 14, 16$ from top to bottom. In (a), (b): $h = 0.5$. In (c), (d): $L = 16$.

(squares) in Fig. 2 (b). Thus, for the chaotic spin model, $t_R \propto D^{1/3}t_{\text{Th}}$, which means that as L increases, the two times get exponentially farther from each other and the hole elongates significantly.

In noninteracting disordered systems, the Thouless time is the diffusion time of a particle through the sample. It is inversely proportional to the Thouless energy, E_{Th} , determined by the diffusion constant and system size [37, 54]. Within the energy scale defined by E_{Th} , the level statistics of these systems follow those from random matrices [54, 55], so the level number variance, Σ^2 , grows logarithmically with the energy interval ℓ , while for level separations larger than the Thouless energy, $\Sigma^2(\ell)$ deviates from this behavior. In random matrix theory, $\Sigma^2(\ell)$ and $b_2(t)$ are both computed from the two-level cluster function [37, 56], so the escape of $\Sigma^2(\ell)$ from the logarithmic curve for $\ell > E_{\text{Th}}$ is related with deviations from universality for times shorter than t_{Th} .

For the interacting disordered system (1), the point where $\Sigma^2(\ell)$ escapes the GOE prediction has also been associated with the Thouless energy [57]. It was shown that E_{Th} decreases with the disorder strength, as the system approaches the many-body localized phase. In Fig. 2 (c), we analyze the relationship between E_{Th} and t_{Th} for various values of h and confirm that $E_{\text{Th}} \propto 1/t_{\text{Th}}$ also for the interacting model.

In Fig. 2 (d), we study the dependence of t_{Th} on the disorder strength. The Thouless time grows exponentially with h and eventually reaches t_R for $h > 2.5$, when

the system localizes and the correlation hole ceases to exist.

Time Scales for the Spin Autocorrelation Function.— An analytical expression for $I(t)$ exists for the GOE model, where the eigenstates $|\psi_\alpha\rangle$ are random vectors and the eigenstate expectation values $I_{\alpha\beta} = \langle\psi_\alpha|I|\psi_\beta\rangle$ are all approximately equal, so $I^{\text{GOE}}(t) \propto P_S^{\text{GOE}}(t)$ [42, 49]. In this case, we recover the results from Eqs. (5) and (6). For realistic systems, on the other hand, $\langle\psi_\alpha|I|\psi_\beta\rangle$ varies with the energy region and a complete expression for $I(t)$ is not yet available. We therefore resort to numerics.

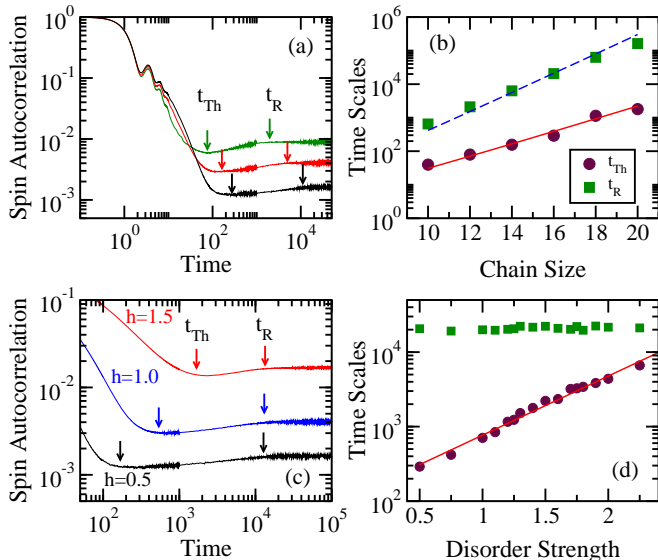


FIG. 3. Spin autocorrelation function vs time in (a) and (c). Thouless and relaxation times as a function of system size (b) and of disorder strength (d). Circles are for t_{Th} , squares for t_{R} . In (b): solid line is for Eq. (8) and dashed line for Eq. (6). In (d): solid line is for the fit $124e^{1.8h}$. In (a): $L = 12, 14, 16$ from top to bottom. In (a), (b): $h = 0.5$. In (c), (d): $L = 16$.

At long times, the behavior of $I(t)$ is similar to $P_S(t)$. As seen in Fig. 3 (a), the correlation hole visibly stretches with system size. The quantitative analysis is done in Fig. 3 (b), which shows that the time to reach the minimum of the hole increases exponentially with L , as in Eq. (8), and the relaxation time follows again Eq. (6). In analogy to the dependence of the survival probability on disorder strength, the minimum of the correlation hole

for $I(t)$ gets postponed to later times as h increases, as illustrated in Fig. 3 (c). This time grows exponentially with h , as shown in Fig. 3 (d), until $t_{\text{Th}} \sim t_{\text{R}}$.

The parallel between the long-time behavior of the survival probability and the spin autocorrelation function demonstrates that $P_S(t)$ is a useful reference for the analysis of more complicated physical observables. This simple quantity, investigated for many decades [58], is easier to study analytically and appears explicitly in the equation of the evolution of any observable. Indeed, for an arbitrary observable O that commutes with H_0 like $I(t)$, we have the direct relation $O(t) = P_S(t)O(0) + \sum_{n,m \neq \text{ini}} \langle n_{\text{ini}} | e^{iHt} | n \rangle \langle n | O | m \rangle \langle m | e^{-iHt} | n_{\text{ini}} \rangle$ [39], where $|n\rangle$ are the eigenstates of H_0 .

Discussion.— Using a detailed picture of the stages involved in the relaxation of realistic interacting many-body quantum systems, we showed that the Thouless time, t_{Th} , and the relaxation time, t_{R} , increase exponentially with system size L . Our analysis was done for the survival probability and the spin autocorrelation function. The results for both quantities are comparable.

In noninteracting disordered systems, the Thouless dimensionless conductance is the ratio $t_{\text{R}}/t_{\text{Th}}$, where t_{Th} is the classical diffusion time. For the interacting chaotic model, we found that $t_{\text{R}}/t_{\text{Th}} \propto e^{L(\ln 2)^3}$. As the disorder strength grows and the system leaves the chaotic region toward localization, the gap between the two time scales decreases and $t_{\text{R}}/t_{\text{Th}} \rightarrow 1$.

The Thouless time in interacting models is the time for the initial state to fully spread in the exponentially large many-body space accessible to it. Beyond that, the dynamics is purely quantum and reaches complete relaxation via the dephasing of the level spacings. The fact that t_{Th} diverges in the thermodynamic limit is consistent with the quantum-classical correspondence principle.

ACKNOWLEDGMENTS

M.S. and L.F.S. are supported by the NSF Grant No. DMR-1603418. E.J.T.-H. acknowledges funding from VIEP-BUAP, Mexico. He is also grateful to LNS-BUAP for allowing use of their supercomputing facility. We are very thankful to Francisco Pérez-Bernal for allowing us to use the supercomputer at the University of Huelva in Spain and for providing technical assistance.

[1] U. Gavish and Y. Castin, Phys. Rev. Lett. **95**, 020401 (2005).
 [2] I. Bloch, J. Dalibard, and W. Zwerger, Rev. Mod. Phys. **80**, 885 (2008).
 [3] B. Gadway, D. Pertot, R. Reimann, and D. Schneble, Phys. Rev. Lett. **105**, 045303 (2010).
 [4] I. Bloch, J. Dalibard, and S. Nascimbène, Nat. Phys. **8**, 267 (2012).

[5] P. Jurcevic, B. P. Lanyon, P. Hauke, C. Hempel, P. Zoller, R. Blatt, and C. F. Roos, Nature **511**, 202 (2014).
 [6] P. Richerme, Z.-X. Gong, A. Lee, C. Senko, J. Smith, M. Foss-Feig, S. Michalakis, A. V. Gorshkov, and C. Monroe, Nature **511**, 198 (2014).
 [7] M. Schreiber, S. S. Hodgman, P. Bordia, H. P. Lüschen, M. H. Fischer, R. Vosk, E. Altman, U. Schneider, and I. Bloch, Science **349**, 842 (2015).

- [8] M. Gärttner, J. G. Bohnet, A. Safavi-Naini, M. L. Wall, J. J. Bollinger, and A. M. Rey, *Nat. Phys.* **13**, 781 (2017).
- [9] K. X. Wei, C. Ramanathan, and P. Cappellaro, *Phys. Rev. Lett.* **120**, 070501 (2018).
- [10] C. Gogolin and J. Eisert, *Rep. Prog. Phys.* **79**, 056001 (2016); J. Eisert, M. Friesdorf, and C. Gogolin, *Nat. Phys.* **11**, 124 (2015).
- [11] F. Borgonovi, F. M. Izrailev, L. F. Santos, and V. G. Zelevinsky, *Phys. Rep.* **626**, 1 (2016).
- [12] L. D’Alessio, Y. Kafri, A. Polkovnikov, and M. Rigol, *Adv. Phys.* **65**, 239 (2016).
- [13] A. Dymarsky, “Bound on eigenstate thermalization from transport,” ArXiv:1804.08626.
- [14] R. Nandkishore and D. Huse, *Annu. Rev. Condens. Matter Phys.* **6**, 15 (2015).
- [15] L. David and L. Y. Bar, *Ann. Phys.(Berlin)* **529**, 1600350 (2017).
- [16] M. Serbyn, Z. Papić, and D. A. Abanin, *Phys. Rev. X* **5**, 041047 (2015); *Phys. Rev. B* **96**, 104201 (2017).
- [17] T. Scaffidi and E. Altman, “Semiclassical theory of many-body quantum chaos and its bound,” ArXiv:1711.04768.
- [18] J. Rammensee, J. D. Urbina, and K. Richter, “Many-body quantum interference and the saturation of out-of-time-order correlators,” ArXiv:1805.06377.
- [19] J. Cotler, N. Hunter-Jones, J. Liu, and B. Yoshida, *J. High Energy Phys.* **2017**, 48 (2017).
- [20] H. Gharibyan, M. Hanada, S. H. Shenker, and M. Tezuka, “Onset of random matrix behavior in scrambling systems,” ArXiv:1803.08050.
- [21] T. Nosaka, D. Rosa, and J. Yoon, “The Thouless time for mass-deformed SYK,” ArXiv:1804.09934.
- [22] A. Chan, A. D. Luca, and J. T. Chalker, “Spectral statistics in spatially extended chaotic quantum many-body systems,” ArXiv:1803.03841.
- [23] F. Borgonovi, F. M. Izrailev, and L. F. Santos, “Exponentially fast dynamics in the Fock space of chaotic many-body systems,” ArXiv:1802.08265.
- [24] A. Peres, *Phys. Rev. A* **30**, 1610 (1984).
- [25] J. M. Deutsch, *Phys. Rev. A* **43**, 2046 (1991).
- [26] M. Srednicki, *J. Phys. A* **29**, L75 (1996).
- [27] P. Reimann, *Phys. Rev. Lett.* **101**, 190403 (2008).
- [28] A. J. Short, *New J. Phys.* **13**, 053009 (2011).
- [29] P. R. Zangara, A. D. Dente, E. J. Torres-Herrera, H. M. Pastawski, A. Iucci, and L. F. Santos, *Phys. Rev. E* **88**, 032913 (2013).
- [30] T. Monnai, *J. Phys. Soc. Jpn.* **82**, 044006 (2013).
- [31] S. Goldstein, T. Hara, and H. Tasaki, *Phys. Rev. Lett.* **111**, 140401 (2013).
- [32] A. S. L. Malabarba, L. P. García-Pintos, N. Linden, T. C. Farrelly, and A. J. Short, *Phys. Rev. E* **90**, 012121 (2014).
- [33] S. Goldstein, T. Hara, and H. Tasaki, *New J. Phys.* **17**, 045002 (2015).
- [34] P. Reimann, *Nat. Comm.* **7**, 10821 (2016).
- [35] L. P. García-Pintos, N. Linden, A. S. L. Malabarba, A. J. Short, and A. Winter, *Phys. Rev. X* **7**, 031027 (2017).
- [36] T. R. de Oliveira, C. Charalambous, D. Jonathan, M. Lewenstein, and A. Riera, *New J. Phys.* **20**, 033032 (2018).
- [37] T. Guhr, A. Mueller-Gröeling, and H. A. Weidenmüller, *Phys. Rep.* **299**, 189 (1998).
- [38] V. V. Flambaum and F. M. Izrailev, *Phys. Rev. E* **64**, 026124 (2001).
- [39] E. J. Torres-Herrera, M. Vyas, and L. F. Santos, *New J. Phys.* **16**, 063010 (2014).
- [40] E. J. Torres-Herrera and L. F. Santos, *Phys. Rev. A* **89**, 043620 (2014).
- [41] M. Távora, E. J. Torres-Herrera, and L. F. Santos, *Phys. Rev. A* **94**, 041603 (2016); **95**, 013604 (2017).
- [42] E. J. Torres-Herrera and L. F. Santos, “Signatures of chaos and thermalization in the dynamics of many-body quantum systems,” ArXiv:1804.06401.
- [43] L. Leviandier, M. Lombardi, R. Jost, and J. P. Pique, *Phys. Rev. Lett.* **56**, 2449 (1986).
- [44] T. Guhr and H. Weidenmüller, *Chem. Phys.* **146**, 21 (1990).
- [45] J. Wilkie and P. Brumer, *Phys. Rev. Lett.* **67**, 1185 (1991).
- [46] Y. Alhassid and R. D. Levine, *Phys. Rev. A* **46**, 4650 (1992).
- [47] T. Gorin and T. H. Seligman, *Phys. Rev. E* **65**, 026214 (2002).
- [48] E. J. Torres-Herrera and L. F. Santos, *Philos. Trans. Royal Soc. A* **375**, 20160434 (2017); *Ann. Phys. (Berlin)* **529**, 1600284 (2017).
- [49] E. J. Torres-Herrera, A. M. García-García, and L. F. Santos, *Phys. Rev. B* **97**, 060303 (2018).
- [50] E. J. Torres-Herrera and L. F. Santos, *Phys. Rev. B* **92**, 014208 (2015).
- [51] M. Schiulaz, M. Távora, and L. F. Santos, “From few-to many-body quantum systems,” ArXiv:1802.08691.
- [52] M. Takahashi, *Thermodynamics of One-Dimensional Solvable Models*, 2nd ed. (Cambridge University Press, Cambridge, UK, 2005).
- [53] We stick to the notation t_{Th} for the parallel with the realistic many-body system, but for the GOE model it does not make sense to call it Thouless time.
- [54] D. Thouless, *Phys. Rep.* **13**, 93 (1974).
- [55] B. L. Al’tshuler and B. I. Shklovskii, *Sov. Phys. JETP* **64**, 127 (1986).
- [56] M. L. Mehta, *Random Matrices* (Academic Press, Boston, USA, 1991).
- [57] C. L. Bertrand and A. M. García-García, *Phys. Rev. B* **94**, 144201 (2016).
- [58] L. A. Khal’fin, *Sov. Phys. JETP* **6**, 1053 (1958); L. Fonda, G. C. Ghirardi, and A. Rimini, *Rep. Prog. Phys.* **41**, 587 (1978).

Appendix A: Time scales for GOE matrices

We give here more detail on how the time for the minimum of the correlation hole and the time for the saturation of the dynamics were derived for GOE matrices, where the elements are real random numbers from a Gaussian distribution with variances 2 (diagonal elements) and 1 (off-diagonal elements). This choice implies that $\Gamma = \sqrt{D}$.

The initial state $|\Psi(0)\rangle$ is an eigenstate of the diagonal part H_0 of the total random matrix H chosen with energy $E_{\text{ini}} = \langle \Psi(0) | H | \Psi(0) \rangle \sim 0$. The eigenstates $|\psi_\alpha\rangle$ of H are random vectors, that is, their components are real random numbers from a Gaussian distribution constrained by normalization. The initial state written in the energy eigenbasis is therefore also a normalized random vector, so the infinite-time average of the survival probability is

$$\overline{P_S} = \sum_{\alpha} |\langle \psi_\alpha | \Psi(0) \rangle|^4 \approx \frac{D}{3}. \quad (\text{A1})$$

1. Time for the Minimum of the Correlation Hole

To obtain Eq. (5) of the main text, we expand to long times the first term of Eq. (4), which involves the Bessel function,

$$D \frac{\mathcal{J}_1^2(2\Gamma t)}{(\Gamma t)^2} \rightarrow \frac{D}{\pi(\Gamma t)^3} \quad (\text{A2})$$

and expand the b_2 function to short times,

$$b_2\left(\frac{\Gamma t}{2D}\right) \rightarrow 1 - \frac{\Gamma t}{D} \quad (\text{A3})$$

Combining the two in the derivative of $P_S(t)$, we have

$$\left. \frac{dP_S(t)}{dt} \right|_{t=t_{\text{Th}}^{\text{GOE}}} = \frac{1 - \overline{P_S}}{D - 1} \left[-3 \frac{D}{\pi \Gamma^3 t^4} + \frac{\Gamma}{D} \right] \Big|_{t=t_{\text{Th}}^{\text{GOE}}} = 0, \quad (\text{A4})$$

from where we find the time for the minimum of the hole,

$$t_{\text{Th}}^{\text{GOE}} \sim \left(\frac{3}{\pi}\right)^{\frac{1}{4}} \frac{\sqrt{D}}{\Gamma} = \left(\frac{3}{\pi}\right)^{\frac{1}{4}} \sim 0.989. \quad (\text{A5})$$

We notice that if the matrix elements are rescaled, as done in Ref. [19] of the main text, so that the width of the density of states is fixed, Eq. (A5) of course changes and $t_{\text{Th}}^{\text{GOE}}$ becomes dependent on D . It is also worth comparing our result with that in Ref. [46], where the expression for $P_S(t)$ does not properly capture the short time decay. As a consequence, it is found incorrectly that $t_{\text{Th}}^{\text{GOE}}$ is analogous to t_{Th} for the real system (Eq. (8) of the main text).

The minimum value reached by the survival probability is $2/D$. This can be seen by using Eq. (A2) and Eq. (A3) in Eq. (4) of the main text, which gives

$$P_S(t)|_{t=t_{\text{Th}}^{\text{GOE}}} \approx \frac{1 - \overline{P_S}}{D - 1} \left[\frac{D}{\pi(\Gamma t_{\text{Th}}^{\text{GOE}})^3} - \left(1 - \frac{\Gamma t_{\text{Th}}^{\text{GOE}}}{D}\right) \right] + \overline{P_S} \sim \frac{1 - \overline{P_S}}{D - 1}(-1) + \overline{P_S} \sim \frac{2}{D}. \quad (\text{A6})$$

2. Relaxation Time

To obtain Eq. (6) of the main text, we expand the two-level form factor to long times,

$$b_2\left(\frac{\Gamma t}{2D}\right) \rightarrow \frac{D^2}{3\Gamma^2 t^2}, \quad (\text{A7})$$

and neglect the term involving the Bessel function, which goes to zero for $t \rightarrow \infty$. Substituting Eq. (A7) into Eq. (4) of the main text, gives us

$$\frac{|P_S(t) - \overline{P_S}|}{\overline{P_S}} \approx \frac{1 - \overline{P_S}}{\overline{P_S}(D - 1)} \frac{D^2}{3\Gamma^2 t^2} \approx \left(\frac{D}{3\Gamma t}\right)^2, \quad (\text{A8})$$

since

$$\frac{1 - \overline{P_S}}{\overline{P_S}(D-1)} \rightarrow \frac{1}{3} \quad (\text{A9})$$

for large D . This shows that $P_S(t)$ approaches the saturation value following a power-law behavior, so the time scale for complete relaxation is not well defined. Yet, one can define the relaxation time as the point where

$$\frac{|P_S(t_R) - \overline{P_S}|}{\overline{P_S}} \sim \delta, \quad (\text{A10})$$

for a small value $\delta > 0$. This gives

$$t_R \sim \frac{D}{3\Gamma\sqrt{\delta}} \Rightarrow t_R^{\text{GOE}} \sim \frac{1}{3\sqrt{\delta}}\sqrt{D}. \quad (\text{A11})$$

3. Numerical Results

To corroborate our analytical predictions, we study the survival probability numerically. In Fig. 4 (a), we plot the analytical expression for $P_S(t)$ for different dimensions of the GOE matrices. The numerical result for $D = 12870$ is also plotted and, apart from fluctuations at long times, the curve is nearly undistinguishable from the analytical expression. For each curve, we mark $t_{\text{Th}}^{\text{GOE}}$ and t_R^{GOE} . To extract $t_{\text{Th}}^{\text{GOE}}$, we minimize $P_S(t)$ numerically. As for t_R^{GOE} , we compute the time at which the relative difference between $\overline{P_S}$ and $P_S(t)$ is equal to $\delta = 0.01$.

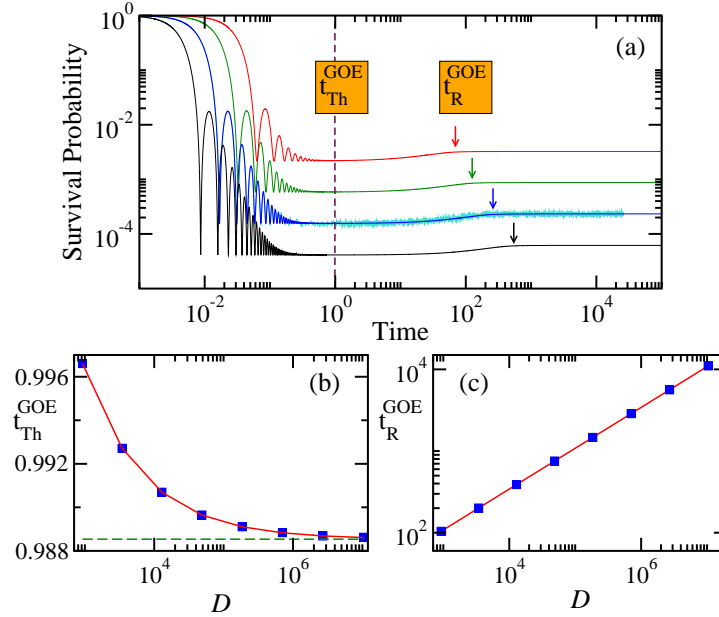


FIG. 4. (a) Analytical expression [Eq. (4) of the main text] for the survival probability as a function of time for GOE matrices of dimensions 924, 3432, 12870, and 48620 from top to bottom. The first three sizes are the same used in Fig.1 (a) of the main text. For $D = 12870$, we also provide the numerical curve averaged over 300 realizations. The time scales $t_{\text{Th}}^{\text{GOE}}$ and t_R^{GOE} are marked for each curve. (b) The time $t_{\text{Th}}^{\text{GOE}}$ for the minimum of the correlation hole as a function of D . The data converge to the asymptotic value $(3/\pi)^{1/4}$ (horizontal dashed line) as $D^{-1/2}$ (solid line). (c) Relaxation time t_R^{GOE} as a function of D . The data follow the behavior $t_R \propto \sqrt{D}$ (solid line) obtained in Eq. (A11).

In Fig. 4 (b) and Fig. 4 (c), we plot the dependence on D of $t_{\text{Th}}^{\text{GOE}}$ and t_R^{GOE} , respectively. We see that $t_{\text{Th}}^{\text{GOE}}$ converges asymptotically to the value given in Eq. (A5), which is indicated with the horizontal dashed line. For small D , the discrepancy is due to finite size corrections. A power-law fitting procedure gives

$$t_{\text{Th}}^{\text{GOE}}(D) - t_{\text{Th}}^{\text{GOE}}(\infty) \sim \frac{0.25}{\sqrt{D}}, \quad (\text{A12})$$

which is shown with the solid line. For t_R^{GOE} , a fitting procedure gives

$$t_R^{\text{GOE}} \sim 3.42\sqrt{D}, \quad (\text{A13})$$

where the prefactor is comparable to $\frac{1}{3\sqrt{\delta}} = 3.33$ predicted by Eq. (A11).